



# Source identification and health risk assessment of heavy metals with mineralogy: the case of soils from a Chinese industrial and mining city

Jun Xu · Yi Wu · Shengli Wang · Yufan Wang · Suhuang Dong ·  
Zhaoming Chen · Liang He

Received: 23 January 2023 / Accepted: 23 March 2023 / Published online: 1 April 2023  
© The Author(s), under exclusive licence to Springer Nature B.V. 2023

**Abstract** Understanding the precise sources of heavy metals (HMs) in soil and the contribution of these sources to health risks has positive effects in terms of risk management. This study focused on the HMs in the soil of five land uses in an industrial and mining city. The sources of HMs in soils were identified, and the soil mineralogical characteristics and health risks of HMs were discussed. The results showed that the HMs (Cu, Zn, Ni, Cd, Pb) found in

the soil of the five land uses were affected by human activities. For example, the Cu in grassland, gobi beach, woodland, green belt, and farmland is 22.3, 3.5, 22.5, 16.7, and 21.3 times higher than the soil background values in Gansu Province, respectively. The Positive Matrix Factorization model (PMF) results revealed that traffic emissions and industrial and agricultural activities were the primary sources of HMs in the soil, with industrial sources accounting for the largest share at 55.79%. Furthermore, various characteristics proved that the studied HMs were closely related to smelting products. Concentration-oriented health risk assessments showed that HMs in the different soil types held non-carcinogenic and carcinogenic risks for children and adults. Contamination source-oriented health risk assessments of children and adults found that industrial activities controlled non-carcinogenic and carcinogenic risks. This study highlighted the critical effects of smelting on urban soil and the contribution of pollution sources to health risks. Furthermore, this work is significant in respect of the risk control of HMs in urban soils.

**Supplementary Information** The online version contains supplementary material available at <https://doi.org/10.1007/s10653-023-01548-1>.

J. Xu · Y. Wu · S. Wang (✉) · Y. Wang · S. Dong ·  
Z. Chen · L. He  
College of Earth and Environmental Sciences, Lanzhou  
University, 222 Tianshui South Road, Lanzhou 730000,  
China  
e-mail: wangshengli@lzu.edu.cn

J. Xu  
e-mail: xujun20@lzu.edu.cn

Y. Wu  
e-mail: ywu2018@lzu.edu.cn

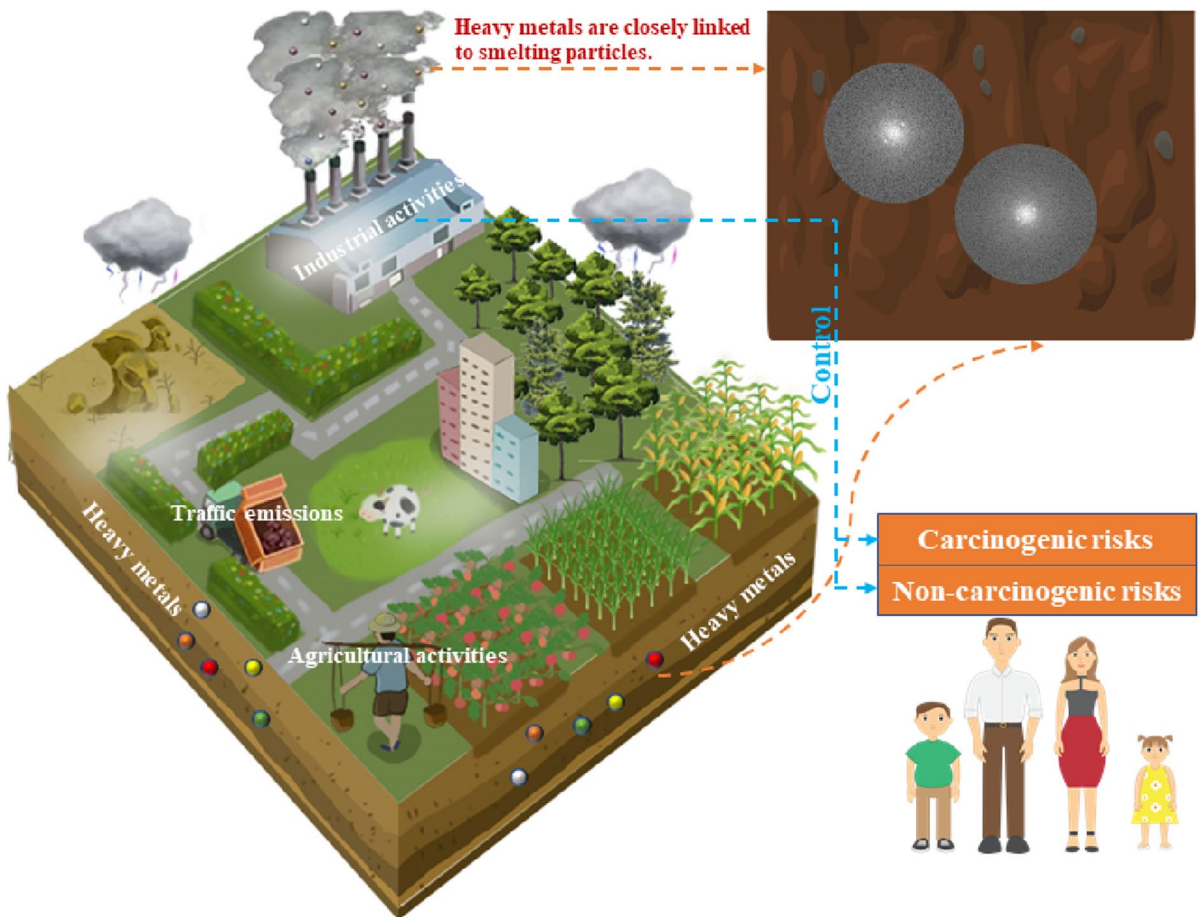
Y. Wang  
e-mail: wangyufan21@lzu.edu.cn

S. Dong  
e-mail: dsharlene@163.com

Z. Chen  
e-mail: chenzhm21@lzu.edu.cn

L. He  
e-mail: lhe2021@lzu.edu.cn

## Graphic Abstract



**Keywords** Heavy metals · Land uses · Sources · Mineralogy · Health risk

### Abbreviations

HMs	Heavy metals	SOM	Soil organic matter
HM	Heavy metal	XRD	X'Pert Pro diffractometer
PMF	Positive Matrix Factorization model	STEM	Scanning transmission electron microscopy
$I_{geo}$	Geoaccumulation index	HRTEM	High-resolution transmission electron microscopy
EF	Enrichment factor	EDS	Energy-dispersive spectrometer
PI	Nemerow pollution index	XPS	X-ray photoelectron spectroscopy
CSI	Contamination safety index	HI	Total exposure hazard index
PCA	Principal component analysis	TCR	Total carcinogenic risk
CA	Cluster analysis	CV	Coefficient of variation
APCS	Absolute Principal Component Scores	AF	SkinAdherence factor
MLR	Multiple Linear Regression	BW	Average body weight
HAR	Human health risk		
EC	Electric conductivity		

## Introduction

Heavy metal (HM) pollution in soil has inspired worldwide concerns owing to its toxicity, persistence, non-biodegradable nature, and the ability to accumulate in the food chain (Ağca & Özdel, 2014; Anaman et al., 2022). According to the first national soil pollution survey results, contaminant concentrations in 16.1% of the soil samples exceeded the standard limit of China's Ministry of Environmental Protection and Ministry of Land and Resources, being mainly inorganic, especially HM pollution (MEPPRC and MLR-PRC, 2014). HM accumulation in soil causes tremendous damage, such as soil function degradation, soil nutrient loss, and food chain contamination, affecting vegetation growth and human health (Fei et al., 2020; Gopinathan et al., 2022b; Xu et al., 2017; Zang et al., 2017b).

Heavy metals (HMs) in soil are originally from natural and anthropogenic sources. The natural source is mainly the parent material (Chen et al., 2016; Lu et al., 2009). The anthropogenic source is the primary source of soil pollution, including metalliferous industries, mining and smelting, agricultural activities, vehicle exhaust, and atmospheric deposition (Cai et al., 2019; Wu et al., 2022). Many studies have focused on soil pollution in farmland and in mining areas (Anaman et al., 2022; Fei et al., 2022; Tian et al., 2022), but rather few studies have investigated the concentration of HMs in soils subjected to different land uses. However, the concentration of HMs in soils varies between land-use types, with different possible hazards to human survival, and there may be different sources of contamination (Huang et al., 2018).

There are many methods used for assessing pollution and sources of HMs in soils. On the one hand, assessments based on geochemical backgrounds such as the geoaccumulation index ( $I_{geo}$ ), the enrichment factor (EF), the Nemerow pollution index (PI), and the contamination safety index (CSI) (Christophoridis et al., 2009; Sutherland, 2000) are used to determine the impact of human activities on the accumulation of HMs in soils. On the other hand, geostatistical models based on geographic information systems, multivariate statistics analyses (principal component analysis, PCA, cluster analysis, CA), and isotopic signatures are often used as qualitative methods to determine pollution sources (Cai et al., 2017; Huang et al.,

2018; Qu et al., 2013). Quantitative methods used in previous source studies have mostly included receptor models, such as PCA-related methods (Absolute Principal Component Scores, APCS, Multiple Linear Regression, PCA-MLR, (A) PCS-MLR, UNMIX model), and PMF (Haghnazar et al., 2022; Shen et al., 2021). In recent years, PMF has been widely used to identify the sources of HMs in water, air, sediment, and soil (Haghnazar et al., 2022; Shi et al., 2022). To better represent the impact of pollution sources on human health risk (HAR), this study used PMF combined with a typical health risk modeling approach (PMF-HAR) for quantitative assessment. Due to the uncertainty of concentrations and evaluation models, it is difficult to use specific pair parameters to assess the health risk of HMs to humans (Hu et al., 2017; Huang et al., 2021). Fortunately, Monte Carlo simulations have enhanced the understanding of the environmental behavior of HMs in terms of health risks through the interval distribution of parameters (Gu et al., 2022; Lian et al., 2022). Therefore, a combination of probabilistic assessment and health risk models was used in this study to assess the concentration-oriented health risks of HMs in soil.

It is worth noting that PMF is based on statistics and the corresponding characteristics of HMs' pollution sources for identification purposes. In recent years, machine learning and artificial intelligence have been widely used in a variety of industries, and they are mostly based on parameters to predict or determine the momentum of the research target (Gautam et al., 2021, 2022; Sharma et al., 2021). Compared with these two emerging methods, PMF is based on the idea of dimensionality reduction analysis, combined with the environmental chemical behavior of pollutants to determine the main sources of pollution; relatively then PMF model can be more scientific to determine the source of pollutants. However, PMF cannot provide direct evidence of pollution sources and thus cannot provide accurate scientific guidance for the risk control scheme of HMs in government departments. Therefore, the results of the PMF should be combined with the characteristics of the soil to progressively identify the main contributors to the major pollution sources. With the deepening of people's understanding of minerals, there has also been considerable development relating to the smelting process (Gopinathan et al., 2022a; Zhou et al., 2020). The environmental impact of the waste

which is released into the surrounding soil during different smelting processes, is a cause for great concern (Gopinathan et al., 2022c; Xu et al., 2023). Literature shows that by-products from smelters are deposited in the soil (Jiang et al., 2022; Zhou et al., 2020). Matte smelting, for instance, is currently the most widely used copper production process. Firstly, chalcopyrite ( $\text{CuFeS}_2$ ) removes impurities such as S and Fe under oxygen-rich and high-temperature conditions and then further oxidizes to obtain coarse copper (Yong-Sohn, 2014). However, under high-temperature conditions, HMs will migrate and transform during the smelting process with the flue gas in the environment (Liu et al., 2019). In addition, the random dumping of waste residue from smelting is also an essential source of HMs in mining soil (Zhou et al., 2020). Toxic HMs in slag and waste gas may be re-released into the environment when environmental conditions (pH, soil organic matter, oxygen reduction potential) change (Zhang et al., 2018; Zhuang et al., 2013). In farmland soils, toxic or harmful HMs tend to penetrate groundwater downward and accumulate in vegetables and crops, leading to increase human health risks (Sobanska et al., 2016; Zhou et al., 2020). In arid regions, the HM pollution effect is particularly prominent. Because of droughts, farmers use industrial wastewater as irrigation which accumulates HMs in the soil (Hu et al., 2011; Huang et al., 2010). Therefore, combining source analysis results with the distribution and dispersion mechanisms of HMs in the soil of industrial cities assists in further identifying the accurate sources of HMs in soil.

Therefore, the main objectives of this study were to: (1) investigate the concentration of HMs in top-soil under different land uses (woodland, grassland, farmland, gobi beach, and green belts) in an industrial and mining city; (2) identify and quantify potential sources of HMs; (3) explore the distribution and dispersion mechanisms of typical HMs in soils; and (4) assess concentration-oriented and source-oriented health risks.

## Materials and methods

### Study area and sampling

Jinchang city ( $37^{\circ}47'–39^{\circ}00'N$ ,  $101^{\circ}04'–102^{\circ}43'E$ ) is located in northwest China, in the middle of Gansu

Province, in the eastern section of the Hexi Corridor, in the northern foot of Qilian Mountain, on the southern edge of Alashan. The area lies in the temperate continental arid climate zone, with an annual average temperature of  $4.8–9.2^{\circ}C$ , a yearly average rainfall of 140–350 mm, and potential evaporation of about 2100 mm, respectively (Kennedy et al., 2011; Li et al., 2016). This area's non-ferrous metal ore reserves are relatively abundant, especially the nickel-based precious metal deposits, so it is known as “China's nickel capital” (Huang et al., 2010). In addition, irrigated agriculture has developed significantly in Jinchang, making it a critical grain production base in northwest China (Xing & Ma, 2021). With the “Western Development Strategy” implemented over the past two decades, agriculture and industry in the region have developed rapidly. However, the soil environment is threatened by various pollutants, especially HM pollution (Guan et al., 2018).

### Soil sampling and analysis

One hundred and sixty-two surface soil samples (0–20 cm deep) were collected from the study area (Fig. 1, in August 2017 and in April 2018), of which the land can be roughly divided into five categories: gobi beach, green belt, grassland, woodland, and farmland, with the number of samples being 55, 41, 20, 32, and 14, respectively. In addition, the number of points used is proportional to the area covered by each land-use type, meaning that more soils are collected for land-use types with a larger area to cover. Considering that the gobi beach is far from urban areas and is less disturbed by human activities, it can be used as a field blank sample for the time being. Sampling was carried out by first removing debris from the soil surface, removing plants and roots, and digging up an area of  $25 \times 25$  cm with a sampling tool to a depth of 0–20 cm. The soil samples were stored in a polyethylene bag and immediately transported to the laboratory. The samples were then air-dried for two weeks at ambient temperature, fully ground, and sieved through a 2-mm mesh to remove coarse debris for measuring electric conductivity (EC) and soil organic matter (SOM). For the determination of HMs, the soil samples were further ground and passed through a 100-mesh sieve before laboratory analysis. The EC was measured in a 1:2.5 sediment solution at room temperature using an EC meter (HI 98,311,

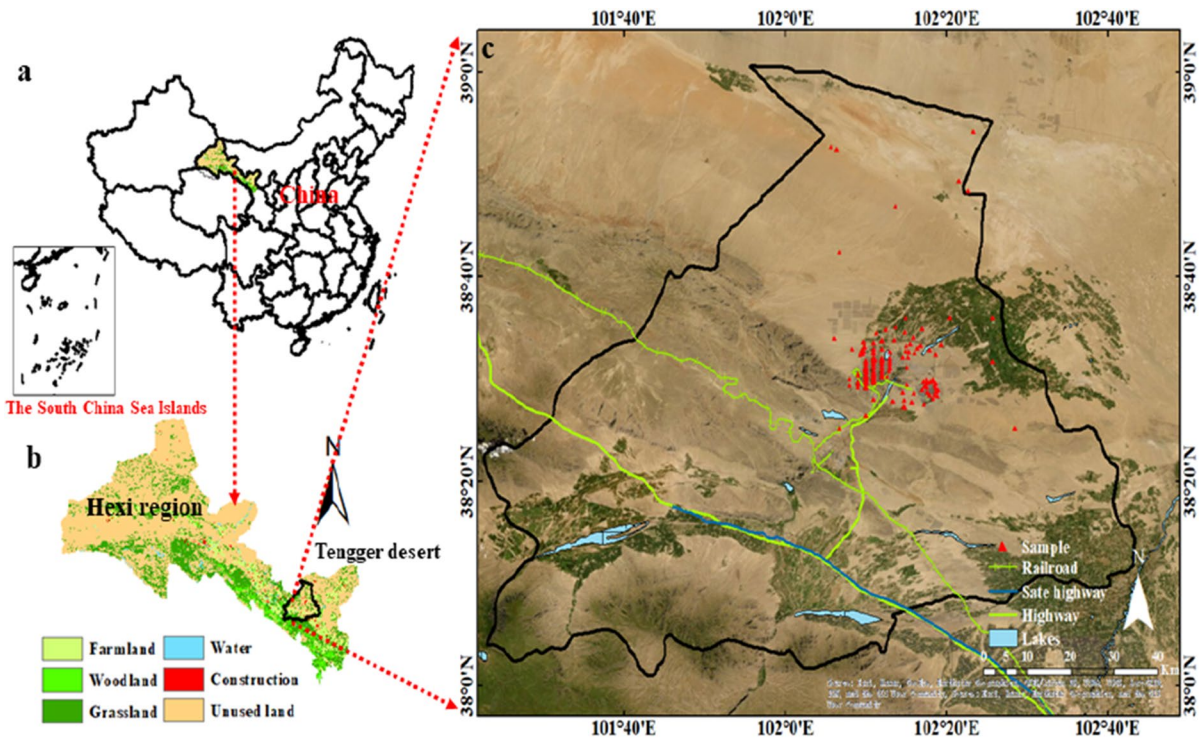


**Fig. 1** Spatial distribution map of surface soil sample points

HANNA Instruments, Italy) (Kavdir & Killi, 2008). SOM was determined by the potassium dichromate oxidation method (Guppy et al., 2005). For HM analysis, 0.5 g of air-dried soil samples was digested in a microwave digestion system (Anton Paar, Multiwave PRO, 180–240 °C) with an acid mixture (3 ml HNO<sub>3</sub>, 1 mL HCl, 1 mL HF, and 1 mL H<sub>2</sub>O<sub>2</sub>) and diluted to 10 ml with deionized water (Zang et al., 2017a). The clear solutions were obtained from the digestion, filtered, reconstituted to the desired volume, and analyzed by atomic absorption spectrophotometry (Thermo Electron, M6MK2, USA).

**Positive matrix factorization model**

The PMF is a new method developed based on factor analysis (Paatero & Tapper, 1993), which is widely used in the source identification of environmental pollutants (Li et al., 2022b; Wang et al., 2021). PMF 5.0, recommended by US EPA, was used to determine the contribution of single HM pollution (USEPA, 2014). The concentration of

HMs can be regarded as *i* multiplied by *j* matrix *X*. Where *i* is the number of samples, *j* is the number of elements and then can be decomposed into factor contribution (*G*) and factor distribution matrix (*F*), the calculation formula is as follows:

$$X_{ij} = \sum_{k=1}^p g_{ik}f_{kj} + e_{ij}$$

*X<sub>ij</sub>* is the concentration of pollutant *i* observed for the *k<sub>th</sub>* time; *j* is the factor; *g<sub>ik</sub>* is the contribution of source *k* in sample *i* (mg/kg); *f<sub>jk</sub>* is the amount of element *j* from source *k*; *p* is the number of HM sources; *e<sub>ij</sub>* is the random error.

The PMF model minimizes the objective function *Q*, and the residual *e<sub>ij</sub>* and uncertainty *u<sub>ij</sub>* of all samples are expressed as follows.

$$Q = \sum_{i=1}^n \sum_{j=1}^m \left( \frac{e_{ij}}{u_{ij}} \right)^2$$

where *u<sub>ij</sub>* is the uncertainty of the *j* HM in the first sample; when the concentration of HMs is greater

than the detection limit (MDL), the uncertainty (Unc) calculation formula is as follows:

$$\text{Unc} = \sqrt{(S \times X)^2 + (0.5 \times \text{MDL})^2}$$

S is the error fraction of chemical analysis, and X is the concentration of HMs.

When the concentration of HMs is less than or equal to MDL, the calculation formula of Unc is as follows:

$$\text{Unc} = \frac{5}{6} \times \text{MDL}$$

### Soil mineralogy analysis

The mineral composition of the mixed soil samples was analyzed by X'Pert Pro diffractometer (XRD, PANalytical, Netherlands). The sample was measured over a range of 5° to 80° (2θ) in steps of 0.002° (2θ) with an integration time of 40 s.

Scanning transmission electron microscopy (STEM, FEI, Tecnai F30, Netherlands) and high-resolution transmission electron microscopy (HRTEM, Tecnai F30, Netherlands) were used for morphological characterization and mineral composition at 200 kV acceleration voltage. The distribution of elements was analyzed by an energy-dispersive spectrometer (EDS) detector.

X-ray photoelectron spectroscopy (XPS, Kratos, Kratos AXIS UltraDLD, UK) was used to determine the morphology and atomic valence of HMs in the soil. For the tests, 20–30 mg powder samples were prepared and sieved over 200 mesh.

### Probabilistic health risk assessment

The health risk assessment model proposed by EPA has been applied in many studies (EPA, 1996, Huang et al., 2018). Ingestion, dermal absorption, and inhalation are the exposure pathways of HMs in soil affecting the human body. The average daily exposure doses (ADDs) of metals in various exposure pathways are calculated as follows (EPA, 1996):

$$\text{ADD}_{\text{ing}} = \frac{C \times \text{IR}_{\text{ing}} \times \text{EF} \times \text{ED}}{\text{BW} \times \text{AT}} \times 10^{-6}$$

$$\text{ADD}_{\text{inh}} = \frac{C \times \text{IR}_{\text{inh}} \times \text{EF} \times \text{ED}}{\text{BW} \times \text{AT} \times \text{PEF}}$$

$$\text{ADD}_{\text{dermal}} = \frac{C \times \text{EF} \times \text{ED} \times \text{AF} \times \text{SA} \times \text{ABS}}{\text{BW} \times \text{AT}} \times 10^{-6}$$

C is the concentration of HMs in surface soil, and its probability distribution is shown in Table S1. The distribution and meaning of the other parameters are shown in Table S2.

The total exposure hazard index (HI) and total carcinogenic risk (TCR) are used to calculate the non-carcinogenic and carcinogenic risks of HMs in soil, respectively. The calculation formula is as follows:

$$\text{HI} = \sum \text{HQ}_i = \sum \frac{\text{ADD}_{ij}}{\text{RfD}_{ij}}$$

$$\text{TCR} = \sum \text{CR}_i = \sum \text{ADD}_{ij} \times \text{SF}_{ij}$$

where RfD is the reference dose of non-carcinogenic pollutants, SF is the slope factor of carcinogenic pollutants, and its value is listed in Table S3. HQ is the non-carcinogenic risk of a single element, and HI is the sum of non-carcinogenic risks of a single element. Non-carcinogenic risk exists when HQ or HI > 1, whereas non-carcinogenic risk is considered small or negligible (Wang et al., 2019). CR and TCR are carcinogenic risks of a single element and total carcinogenic risks, respectively. Cancer risk is acceptable when  $10^{-6} < \text{CR} < \text{TCR} < 10^{-4}$  (Dutta et al., 2022). When CR or TCR >  $10^{-4}$ , there is a significant cancer risk (Dutta et al., 2022). When CR or TCR <  $10^{-6}$  there is no potential cancer risk (Başaran, 2022).

In order to avoid overestimating or underestimating health risks, this study adopted the probabilistic risk method (Monte Carlo simulation) to assess the uncertainty of health risk results (Huang et al., 2021). To furthermore understand the contribution of HM pollution sources in the soils with different land uses to human health risks, the results of PMF were quantified. Specifically, the health risk assessment value was multiplied by the contribution value

of each pollution source to calculate the source-oriented health risk (Huang et al., 2018).

#### Quality control and quality assurance

All glassware and plastic containers were soaked in 10% (v/v)  $\text{HNO}_3$  for at least 24 h and thoroughly cleaned with deionized water before utilization. All reagents and chemicals were of the guaranteed reagent. For quality control and assurance, reagent blanks, the standard reference soil samples (GSS-8) from the Center of National Standard Reference Material of China, and duplicate samples were measured. The mean recoveries of total concentration were 91–108%, and for Cu, Zn, Cd, Pb, and Ni, the relative standard deviation was below 5%. Blank samples were also applied in all the experiments. Duplicate samples were performed simultaneously for 20% of soil samples, and the analytical precision for replicate samples was within  $\pm 10\%$ .

#### Statistical analysis

The normality and homoscedasticity of the data was verified prior to statistical analysis. The means and standard deviations in this paper were calculated using Microsoft Office Excel for 2016 (Microsoft, USA). Pearson correlation coefficient was performed by SPSS 23.0 version (International Business Machines Corporation, USA). Origin 2021 (OriginLab, USA) was used to draw box plots, correlation heat maps, bar charts, and line plots. Monte Carlo simulations were performed using Crystal Ball v11.1.24 (Oracle, USA, Website: <https://www.oracle.com/cn/applications/crystalball/>) software by considering 10,000 iterations at a 95% confidence level to obtain stable risk output (Anaman et al., 2022).

## Result

#### The statistical analysis of heavy metals in soil

The average values of Cu, Zn, Ni, Pb, and Cd in the soil of five land uses exceeded the soil background values of Gansu Province and Hexi Corridor (Guan et al., 2018), indicating that the soil in the study area was affected by human activities (Table 1). As shown in Fig S1, the enrichment of Cu and Ni was higher

than that of other elements. For example, the Cu of grassland, gobi beach, woodland, green belt, and farmland was, respectively,  $22.3 \pm 28.6$ ,  $3.5 \pm 1.2$ ,  $22.5 \pm 21.0$ ,  $16.7 \pm 11.2$ , and  $21.3 \pm 21.4$  times higher than the soil background value in Gansu Province. The distribution of HM pollution in soil with different land uses was distinctive. For example, the distribution of the average value of Cu was woodland > grassland > farmland > green belt > gobi beach. Zn was woodland > green belt > farmland > grassland > gobi beach, indicating that the distribution of HM pollution was related to soil utilization. It is worth noting that there was little difference in the exceeding rate of HMs in soil, which was between 40 and 100%. For example, in all soil samples of grassland, Cu (100%), Zn (90%), Ni (95%), Pb (100%), and Cd (95%) exceeded the corresponding soil background values in Gansu Province.

#### Source apportionment of heavy metals

The results showed a significant correlation between HMs in the soil of five land uses (Table S4). For instance, Cu from grassland and farmland significantly correlated with Ni and Pb; Cu from gobi beach and the green belt significantly correlated with Zn, Ni, Pb, and Cd; and woodland's Cu significantly correlated with Ni, Pb, and Cd. The correlation between these elements indicated that they might share the same source (Huang et al., 2018; Luo et al., 2022). It is noteworthy that the correlation of HMs in the soil of each land use was not the same (Table S4). In addition to farmland, SOM in other land-use soils had a significant indigenous correlation with HMs.

The HMs in the soil for different land uses may have the same pollution sources, and the study area can be used to analyze the sources of HMs in all soil samples. As shown in Fig. S2, Cu and Ni, Pb and Cd in the soil had significant correlations, Zn and Ni had significant correlations with Pb and Cd, and Pb and Cd also had substantial correlations. A model was needed to validate the hypothesis to identify pollution sources accurately.

Three pollution sources and the factor distribution determined by the model are shown in Fig. 2. PMF model data sources included concentration data (162 soil samples, five HMs) and uncertainty files. The signal-to-noise ratio (S/N) of all elements in the model was greater than 1, and the categories of

**Table 1** Statistical summary of heavy metals and physicochemical properties of different land use (HMs: mg/kg; SOM: g/kg; EC: mS/m)

Land use		SOM	EC	Cu	Zn	Ni	Pb	Cd
Grassland, <i>n</i> = 20	Max	61.66	1200.00	3349.85	427.70	1607.51	88.46	0.88
	Min	8.25	133.00	44.11	54.56	35.05	19.75	0.11
	Mean	32.12	331.20	537.29	122.57	313.85	38.34	0.36
	SD	16.07	286.90	688.98	78.40	346.12	18.58	0.20
	CV (%)	50.04	86.63	128.23	63.96	110.28	48.46	57.19
Gobi beach, <i>n</i> = 55	Max	31.36	2120.00	793.56	251.41	1337.29	29.61	0.45
	Min	3.55	93.00	24.40	49.98	20.83	15.65	0.08
	Mean	9.97	411.78	83.79	76.10	92.70	19.67	0.15
	SD	2.88	382.48	30.07	18.13	25.64	1.42	0.05
	CV (%)	28.85	92.88	35.89	23.82	27.66	7.20	33.72
Woodland, <i>n</i> = 32	Max	84.91	3725.00	1735.87	630.62	2603.89	171.85	6.09
	Min	8.58	124.00	42.64	57.75	36.99	9.61	0.08
	Mean	32.24	789.66	541.90	163.57	522.26	35.08	0.69
	SD	17.37	958.30	505.09	139.42	592.49	28.31	1.04
	CV (%)	53.88	121.36	93.21	85.24	113.45	80.69	149.81
Green belt, <i>n</i> = 41	Max	67.57	3999.00	1148.63	654.58	941.59	95.32	1.68
	Min	10.24	100.00	55.36	69.29	58.69	13.94	0.09
	Mean	28.43	756.22	402.04	157.13	319.02	31.23	0.36
	SD	13.14	1234.45	270.77	147.73	237.81	17.30	0.32
	CV (%)	46.22	163.24	67.35	94.02	74.55	55.40	87.70
Farmland, <i>n</i> = 14	Max	67.89	3999.00	1464.73	881.09	2178.17	29.43	1.81
	Min	7.40	118.00	52.90	52.38	49.07	2.35	0.14
	Mean	24.96	1100.00	513.97	156.69	539.07	20.56	0.42
	SD	16.28	1340.46	515.59	209.59	641.57	6.45	0.47
	CV (%)	65.25	121.86	100.32	133.76	119.01	31.39	111.85
Study area, <i>n</i> = 162	Max	84.91	3999.00	3349.85	881.09	2603.89	171.85	6.09
	Min	3.55	93.00	24.40	49.98	20.83	2.35	0.08
	Mean	23.07	623.12	347.99	126.59	300.71	28.02	0.36
	SD	15.93	880.95	438.28	121.56	418.81	18.00	0.54
	CV (%)	69.05	141.38	125.95	96.03	139.28	64.25	151.32
Background value <sup>a</sup>		NA	NA	24.10	68.50	35.20	18.80	0.12
Hexi corridor <sup>b</sup>		NA	NA	35.20	75.34	24.45	5.54	NA

<sup>a</sup>(CNEMC (China National Environmental Monitoring Center), 1995); <sup>b</sup>Average background value of Hexi Corridor (Guan et al., 2018, 2019); NA: Data not available

Cu, Zn, Ni, Pb, and Cd were set to ‘Strong.’ When the pollution source factor was set to 3, the *Q* value was the smallest and most stable, and the results of selecting the minor *Q* (Robust) value were analyzed 20 times. The model fitting ( $R^2$ ) of Cu, Zn, Ni, Pb, and Cd was 0.8052, 0.9910, 0.9225, 0.9994, and 0.8124, respectively—all higher than 0.8. Therefore, the model parameter setting was reliable.

The weights of factor 1, factor 2, and factor 3 were 32.58, 55.79, and 11.63%, respectively (Fig. 2b). In factor 1, Pb was the main load element and the contribution rate was 93.24%. The contribution rates of Cu and Ni in factor 2 were 69.24 and 68.80%,

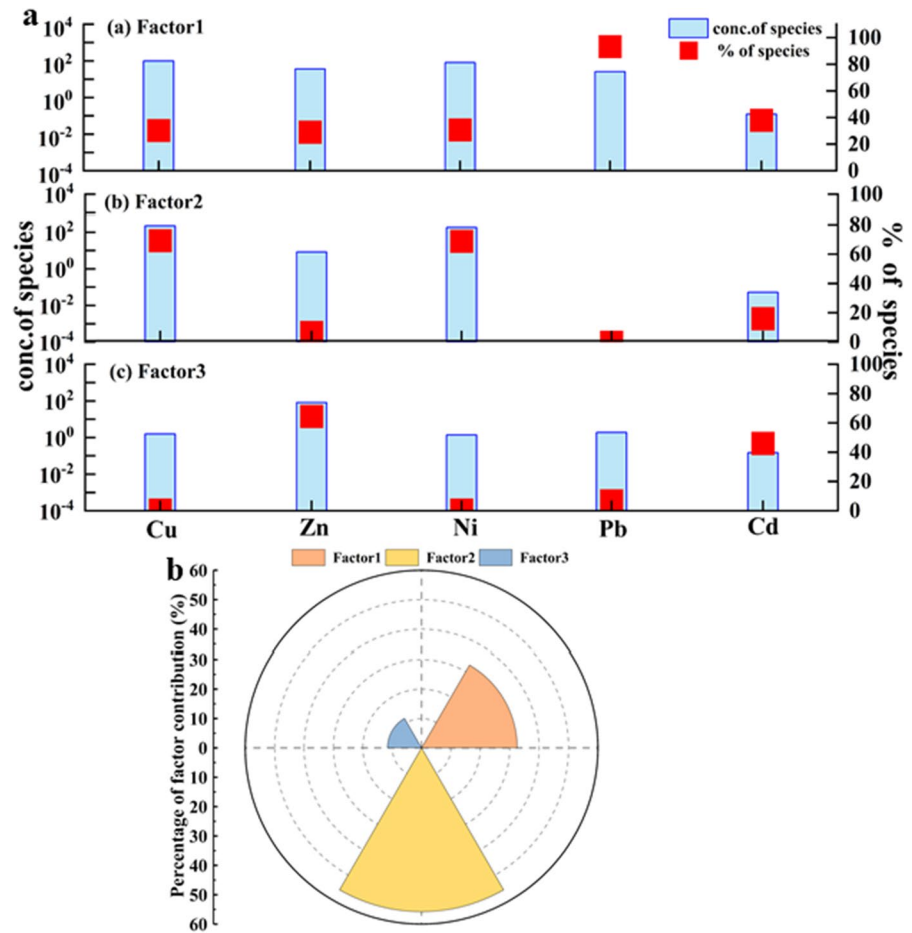
respectively. In factor 3, Zn and Cd were the main load elements, with 64.42 and 46.05% contribution rates, respectively.

#### Mineralogical characterization

According to the results of XRD (Fig. 3), the main mineral phases of soil in five land uses were muscovite, gypsum ( $\text{CaSO}_4$ ), quartz ( $\text{SiO}_2$ ), calcite ( $\text{CaCO}_3$ ), cuprite ( $\text{Cu}_2\text{O}$ ), and hematite ( $\text{Fe}_2\text{O}_3$ ), and the diffraction peak intensity of  $\text{SiO}_2$  was higher than that of other mineral phases. To determine the



**Fig. 2** Heavy metal source apportionment and factor contribution ratios in soils, a: the figure shows the results of PMF source apportionment, b: the figure shows the contribution of each factor



pollution of HMs, STEM-EDS analysis was performed on typical contaminated soil. The distribution of Cu, Ni, O, and Fe in the soil of woodland and farmland was similar to micron-level particles, and the distribution in farmland was more obvious (Fig. 4). In addition, the contents of Cu, Ni, and Fe were highly abundant. Further analysis by fast Fourier transform (FFT) and high-resolution transmission electron microscopy (HRTEM) showed that soil mineral phases in woodland and farmland included Cu<sub>2</sub>O and Fe<sub>2</sub>O<sub>3</sub> (Fig. 4). XPS spectra of Cu 2p and Ni 2p in the soil samples from woodland and farmland are shown in Fig. 5. The results showed that the binding energies of Cu in the woodland and farmland soil samples were 932.51 eV and 932.41 eV, respectively, and the corresponding binding energies of Cu<sub>2</sub>O and Ni were 853.91 eV

and 853.81 eV, respectively, corresponding to Ni<sub>2</sub>O<sub>3</sub>.

### Probabilistic health risks assessment

The non-carcinogenic probability risk of HMs in soils with different uses was evaluated by means of Monte Carlo simulation (Fig. 6). The results showed that adults and children had non-carcinogenic risks for HMs in all land-use soils. The average HI values of children and adults followed the following patterns: woodland > farmland > grassland > green belt > gobi beach. In addition, the non-carcinogenic risk of children was higher than that of adults. The non-carcinogenic probability of HMs in gobi beach was 10%, and the other four land uses were about 30% (Table S5). Therefore, the HMs in grassland, woodland, green belt, and farmland soil had a greater non-carcinogenic

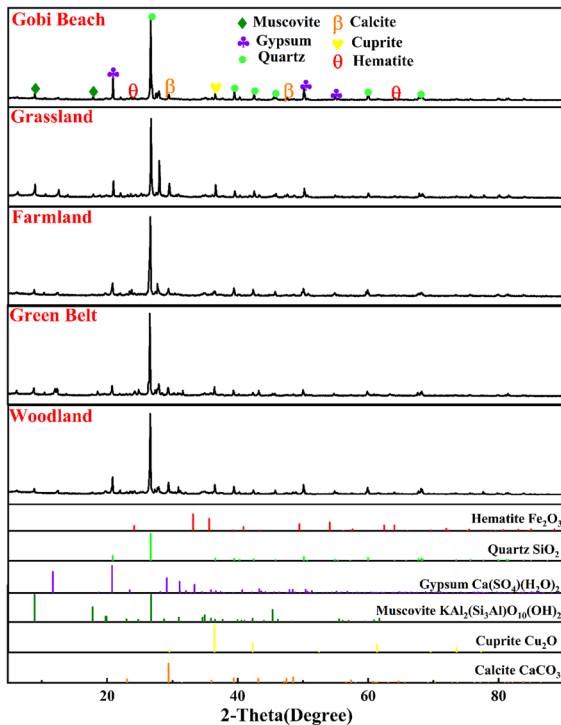


**Fig. 3** XRD-based mineralogy of soil samples from five land-use types

risk and needed to be measured to control. It is worth noting that Cd, Cu, Zn, and Pb had low non-carcinogenic risks for children and adults, and Ni was the main contributor to non-carcinogenic risks.

The average TCR values of children and adults were greater than  $1.0E-04$  (Fan et al., 2021), which was not within the acceptable range of risk (Fan et al., 2021), indicating that HMs in the soil of five land uses all had carcinogenic risks. In addition, the average TCR values of children and adults adhered to the following order: farmland > woodland > grassland > green belt > gobi beach (Fig. 7), which is consistent with the distribution order of non-carcinogenic risk. Cd and Pb in the soil of five land uses did not pose carcinogenic risks to humans. In addition to gobi beach, the carcinogenic probability of Ni to children and adults in other land-use soils exceeded 90% (Table S5). The results of the Monte Carlo simulation for the total carcinogenic risk showed that Ni is the main source of human carcinogenic risk for both children and adults. Although gobi beach is less disturbed by human activities, the carcinogenic risk of HMs cannot be ignored.

## Discussion

Pollution and source apportionment of heavy metals in soil

Coefficient of variation (CV) is normally used to reflect the degree of human disturbance to the environment (Jing et al., 2018). Except for gobi beach, Cu, Zn, Ni, Pb, and Cd in other land uses seem to be affected by severe human activities (Table 1). Although the HMs in gobi beach were less affected by human activities, the average concentration still exceeded the soil background value in Gansu Province (Table 1). It is worth noting that the reserves of Cu and Ni in Jinchang ranked first and second in China, respectively. Therefore, it can be inferred that HMs in gobi beach may mainly stem from the soil's parent material layer. From a global perspective, the concentrations of Cu and Ni in the soil in this study were equivalent to those in Ezhou city, which was also a copper mine city, and other elements were at a medium pollution level (Table S6). However, longitudinally, in addition to Pb, the concentrations of HMs in green belt and farmland in this study were higher than those indicated in Ding et al. (2008) and Huang et al. (2010), especially Cu and Ni (Table S6). Jinchang city is located on the edge of the Tengger Desert and Badain Jaran Desert, where dust events occur frequently. Guan et al. (2017) showed that the concentration of  $PM_{10}$  in the region caused by a dust storm was 43 times that of non-dust storm areas. In addition, from 2017 to 2018, Luo et al. (2022) studied HM pollution in key cities in northwest China. The results showed that the concentrations of Cu, Zn, Ni, and Pb in dust storms in Jinchang city were 172.1, 116.9, 157.9, and 42.0 mg/kg, respectively, and the concentrations of Cu and Ni were the highest in Jinchang city. It has been reported that smelting flue gas is the main source of atmospheric particulate matter in Jinchang city during dust storms, and the dustfall is 2–3 times that of the non-dust storm periods (Zhao, 2012). Concentrations of particulate matter increase significantly during the dust period, coupled with its large specific surface area, which makes it easier to adsorb HMs and then settle on the surface of the land, lakes, plant leaves, and buildings under the action of gravity and airflow (Bisht et al., 2022; Gautam, 2020). Therefore, the exchange of HMs between the atmosphere and soil caused by dust storms in this

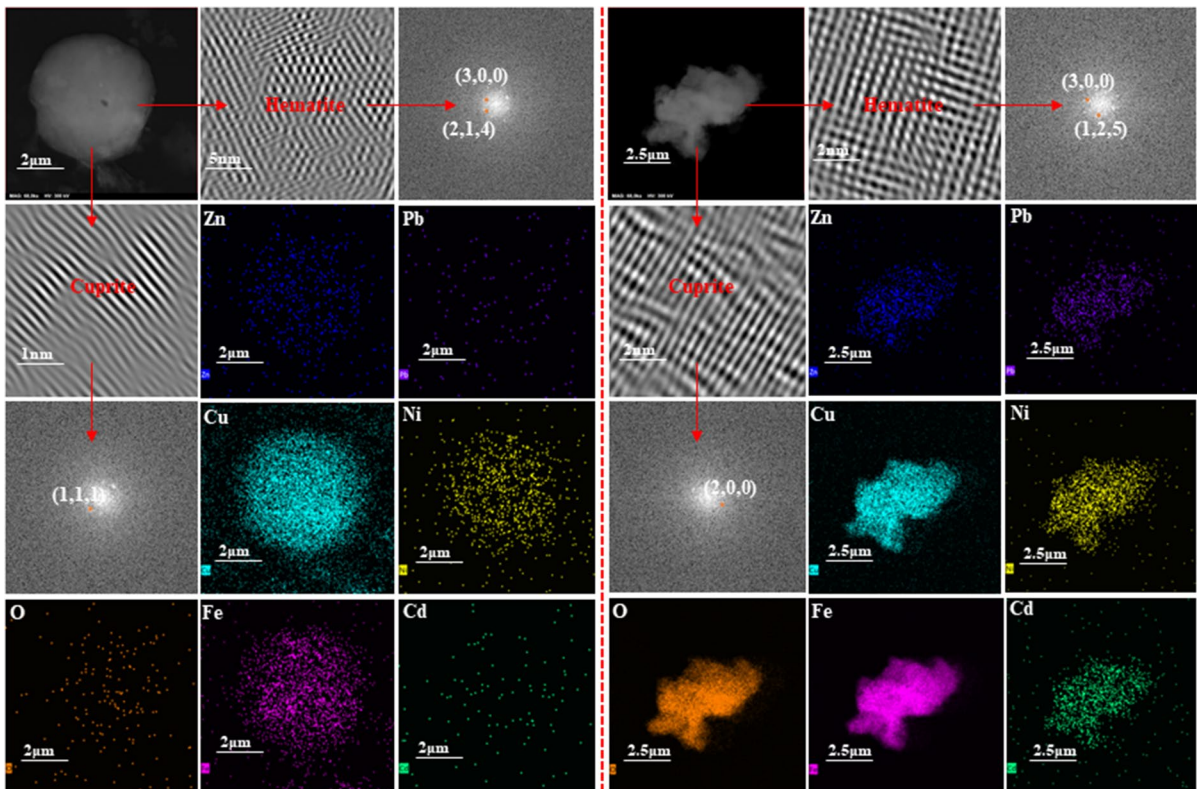


**Fig. 4** STEM-EDS characterization of soils collected from woodland soil (left) and farmland soil (right)

area is more frequent and intense, which is also an essential reason for the increase of Cu and Ni concentrations in the soil of Jinchang city.

The results of the PMF model showed that there were three primary sources of HMs in the study area, and Pb was the main load element of factor 1 (Fig. 2). In the past few decades, tetraethyl lead was added to fuel to reduce the engine knock, and Pb was discharged into the environment with traffic emissions (Liu et al., 2014). Despite the introduction of lead-free gasoline in recent years, Pb has a longer half-life in the environment (Lee et al., 2006), and brake wear is considered to be the primary source of Pb in the environment (Smichowski et al., 2007). Transportation is also more frequent in Jinchang city. As of 2018, the total mileage of highway traffic in the city was 2975.287 km, the freight volume was 1660.37 million tons, and the freight turnover was 332.74 million tons (JCBS, 2018). Therefore, factor 1 is identified as a traffic pollution source. Factor 2 accounts for the largest proportion of Cu and Ni, the main

load elements. Studies have shown that agricultural activities are an important source of Cu in soil and are often used as feed additives to prevent diseases in livestock and poultry (Gupta et al., 2014; Zhang et al., 2021b). In addition, Ni in soil mainly flows from the crust (Chen et al., 2016). However, in this study, Cu and Ni were highly enriched in soil samples. Jinchang is the main city of Cu and Ni mining and smelting in China, and Cu and Ni have a significant correlation (Fig. S2). It can be inferred that factor 2 is an industrial pollution source, which differs from the conclusions of other researchers (Huang et al., 2018; Liu et al., 2022; Zhang et al., 2021b). Therefore, when using PMF to analyze the source of HMs, we should not only consider the unique source of characteristic elements but also combine it with the local economic and social development to determine the source of pollution. Factor 3 has a minor proportion and Zn and Cd are the main load elements. Literature shows that Zn has been widely used as a heat stabilizer in pesticides, fungicides, and plastic films (Shao et al.,

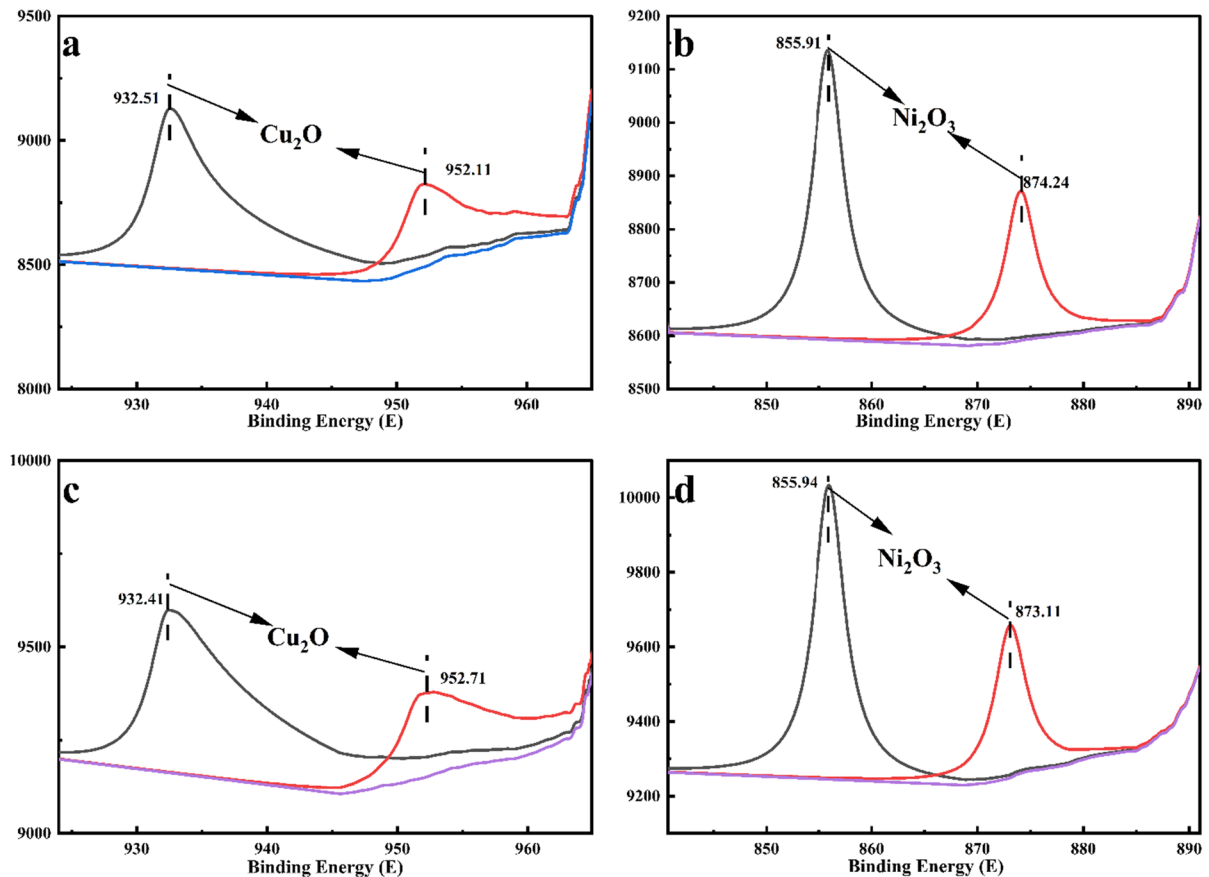


**Fig. 5** XPS spectra (Cu, Ni) of soil samples collected in woodland **a, b** and farmland **c, d**

2016; Wang et al., 2020). Cd is a characteristic element of phosphate fertilizer (Kratz et al., 2016; Liu et al., 2022). In addition, in this study, there was a significant correlation between Zn and Cd ( $r=0.576$ ,  $P \leq 0.05$ , Fig.S2). Therefore, factor 3 can be considered as an agricultural source.

#### Soil mineralogical characteristics

The PMF model results reflected that the main sources of HMs in soil were traffic emissions and industrial and agricultural activities. It is worth noting that the industrial pollution source right is more than 50%, indicating that the HM pollution in the study area is mainly related to industrial activities such as mining, smelting, and coal burning. With researchers' deepening understanding of HM pollution, the distribution of HMs in micron-sized particles plays an important role in earth catalysis

and dynamics (Lefticariu et al., 2017; Zhou et al., 2020). The existence of hematite ( $\text{Fe}_2\text{O}_3$ ) was found at (3,0,0), (1,2,5), and (2,1,5) (Fig. 4). Interestingly, cuprite ( $\text{Cu}_2\text{O}$ ) was found at (1,1,1) and (2,0,0) diffraction points. XRD results also showed the existence of these two minerals (Fig. 3). It has been reported that micron hematite ( $\text{Fe}_2\text{O}_3$ ) is important in non-ferrous metal smelting (Jiang et al., 2022). Xu et al. (2022) also found  $\text{Fe}_2\text{O}_3$  in the soil around the lead (Pb)/zinc (Zn) smelting area. It is worth noting that  $\text{Cu}_2\text{O}$  is usually the intermediate product of refined smelting copper with chalcopyrite ( $\text{CuFeS}_2$ ) as raw material (Sohn et al., 2005). Thus, intensive smelting activities lead to the accumulation of iron oxides and smelting intermediates in soil, which can also reflect the pollution of HMs from the side (Vodyanitskii & Shoba, 2015). Currently, the main raw material for smelting Cu and Ni is sulfide ore, which is smelted by means of a

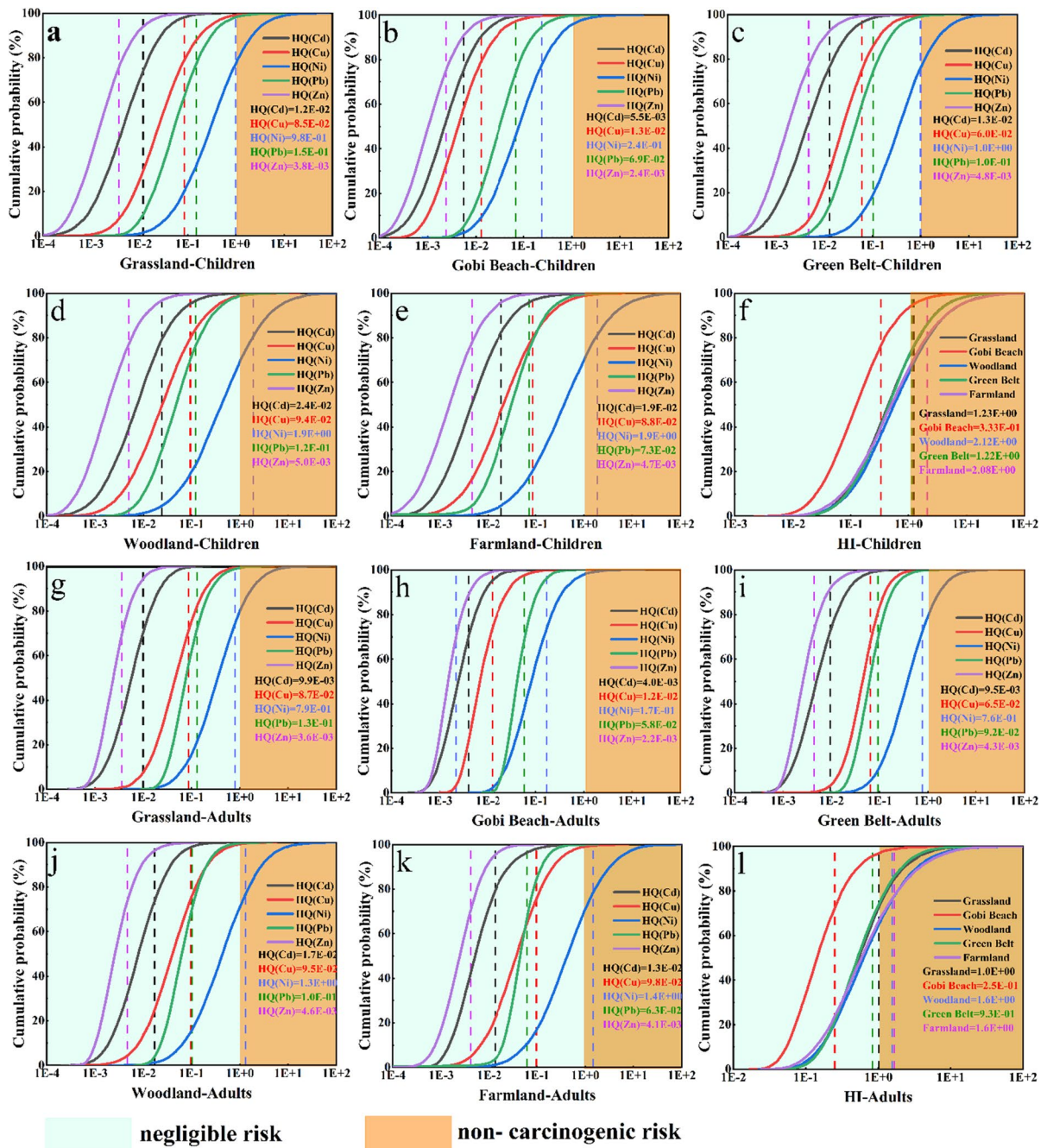


**Fig. 6** The probability distribution for hazard index (HI) and hazard quotient (HQ), and the dotted line in the graph is the mean line

matte smelting process (Crundwell et al., 2011, 2014). Combined with the XPS results of Cu and Ni

(Fig. 5), the mechanism can be explained by the following chemical equations:

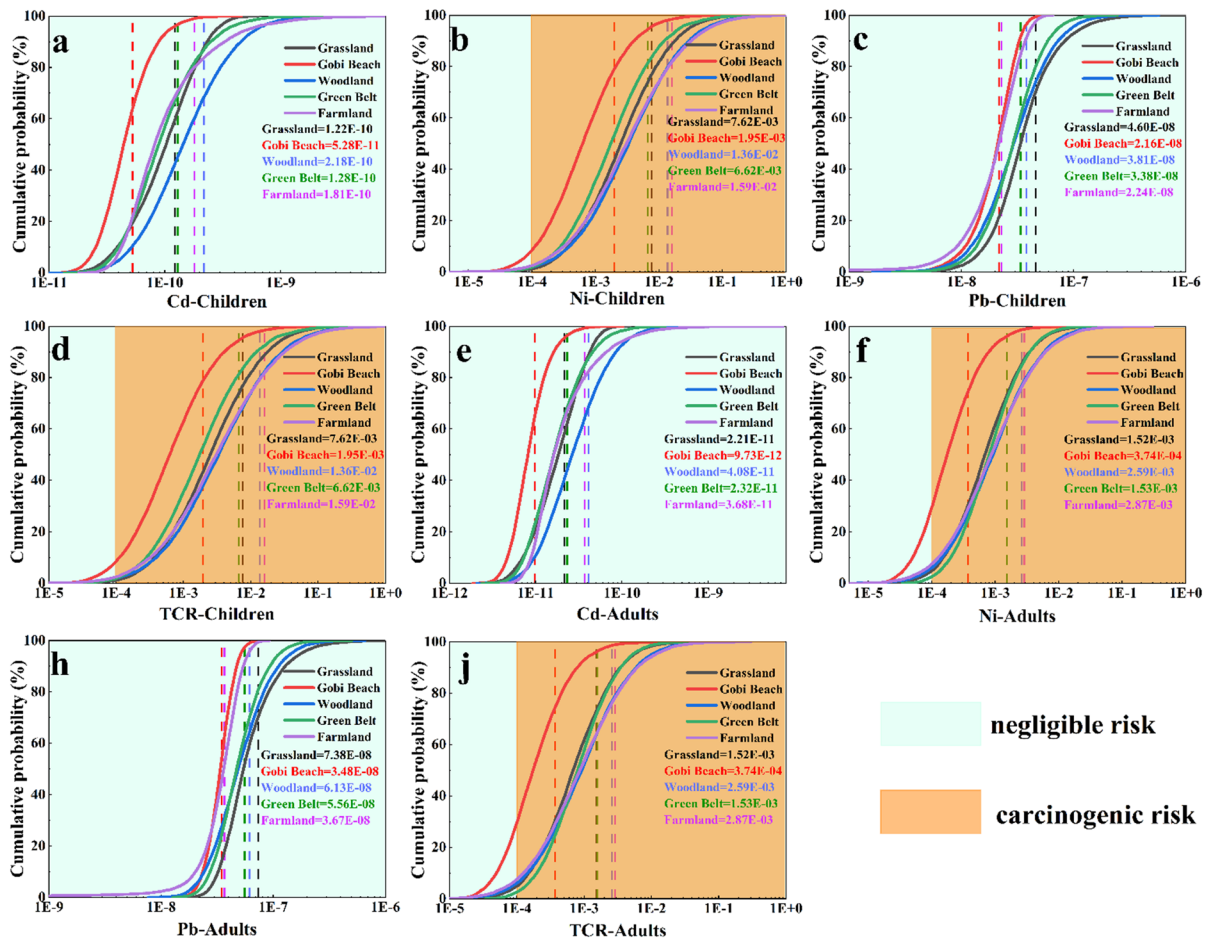
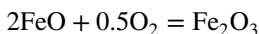
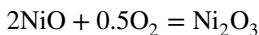
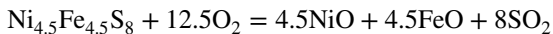
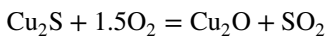


**Fig. 7** The probability distribution and the percentage surpassed  $1E-06$  for total carcinogenic risk (TCR) and carcinogenic risk (CR) index; the dotted line in the graph is the mean line



The smelting temperature of Cu and Ni is 1250 and 700 °C, respectively, which produces Cu and Ni deposits in the soil with the emission of dust in the smelting process. Therefore, it can be concluded that HMs from smelter waste are transferred to soil.

Combined with the results of the PMF model, it can be further proved that ore smelting via industrial activities is an essential source of HM accumulation in soil. In addition, the complexity and reactivity of soil systems lead to the migration of HMs to deep soil, which causes irreversible damage to the polluted groundwater environment in arid areas.

Environmental effects of heavy metals

Overall, HMs in this study area have not only non-carcinogenic but also carcinogenic risks. In addition, the health risk of children is higher than that of adults, since children are in a stage of rapid development and have weak resistance, and are therefore more vulnerable to external influences (Chen et al.,

2022). Ni is an essential trace element for the human body. Exceeding the standard will cause liver injury, cardiopulmonary function injury, and contact dermatitis (Kulikowska et al., 2015; Shentu et al., 2022). Thus, the risk control of soil Ni should be strengthened and measures such as optimizing the industrial structure, strictly controlling the emission of new pollutants, and improving the comprehensive management of HM pollution sources should be implemented. The exposure uptake biodynamics model was combined with the health risk probability model to further explore the impact of the exposure risk model on health risk assessment results. The sensitivity analysis results are shown in Fig. S4. It was found that the non-carcinogenic and carcinogenic risks to children and adults were mainly controlled by the SkinAdherence factor (AF) and the concentration of Ni. Furthermore, there was a significant correlation between the two and the risk value (Table S7), reflecting the parameters' influence on the model results. Therefore, local residents can use wireless devices and masks to reduce direct contact with soil HMs (Ren et al., 2021). Usually, average body weight (BW) has a negative impact on health risk assessment (Chen et al., 2022; Pirsaeheb et al., 2021; Zhang et al., 2021a), and the effect of BW in this study can thus be ignored due to the high concentration of Ni. Gobi beach is a potential source of dust, and according to the analysis in Sect. Probabilistic health risks assessment, the health risks posed by HMs in the soil cannot be ignored. Jinchang city is located in the Hexi Corridor of China in an area with a high incidence of sandstorms. Numerous studies have been conducted worldwide on the relationship between dust and human health, indicating that long-term exposure to dust can lead to respiratory problems, conjunctivitis, skin irritation, and other diseases (Luo et al., 2022; Tao et al., 2012). Pesticides, HMs, organic pollutants, and radioisotopes carried by industrial park emissions and automobile exhaust cannot only be adsorbed on the surface of particulate matter under the action of atmospheric circulation (Almeida-Silva et al., 2013; Khuzestani & Souri, 2013). Photochemical reactions between pollutants and active substances on the surface of particulate matter pose health risks to people along the way (Li et al., 2022a). Therefore, the dust in gobi beach potentially impacts human health and this can be addressed by planting protective forests on the edges of the gobi beach. Studies have shown

that plant and animal uptake of HMs depends mainly on bioavailability (Adamo et al., 2014; Zhang et al., 2018). The HMs carried by the surface dust enter the lungs and stomach of the human body and transform into bioavailability. Different animal evaluation models, evaluation indexes, bioavailability, and ground praise dust affect the study of soil HM and health risks in Jinchang city. Therefore, the use of the Monte Carlo simulation method in this study, considering uncertainties, is crucial to determine the real health risks of HMs. The main point to note is that waste from smelters can be transferred to the surrounding soil in a variety of ways, which means that minerals carried by smelter fumes can enter the body directly. Secondly, minerals deposited on the ground surface can also enter the human body in the presence of surface dust. However, unlike HMs in environmental media such as water and soil, HMs in minerals are more concentrated and toxic (Xu & Fu, 2022), posing an even greater threat to human health.

A PMF-HRA comprehensive evaluation model was developed (based on PMF and HRA models) to understand the contribution of pollution sources to the health risk sources of HMs in soil with different land uses. The normalized contribution value of HM pollution sources based on the PMF model is shown in Fig. S3. The hazards of three pollution sources (traffic emissions, industrial activities, and agricultural activities) to human health under different land uses are outlined in Fig. S5. The contribution of different sources to health risk was similar in children and adults, which is consistent with the findings of other studies (Huang et al., 2021; Ma et al., 2018). In five land use, the non-carcinogenic risks of children and adults are mainly affected by industrial activities. Furthermore, industrial activities were the main carcinogenic risk factors for adults and children (Fig. S5). This indicates that industrial activities have a significant impact on human health risks. It is worth noting that the analysis in Sect. The statistical analysis of heavy metals in soil shows that Cu and Ni far exceed the background values for soils in Gansu Province. In addition,  $\text{Ni}_2\text{O}_3$  and  $\text{Cu}_2\text{O}$  can be observed at the micron level of soil particles, which is a greater threat to human health and ecology. Thirdly, Cu and Ni are the main load elements of factor 2 (industrial activities) and are major contributing element to health risk. Finally, combined with the results of other researchers' studies on HMs in soils (agricultural,

residential, mining, etc.) and atmospheric particulate matter from different areas of the district area (Tong, 2012; Xiaohu et al., 2009; Xiaona et al., 2011; Yuan et al., 2009), both Cu and Ni were found to be the most dominant contaminating elements. Therefore, Cu and Ni can be identified as priority contaminants for further risk control.

In summary, quantifying the contribution of different pollution sources to health risks is conducive to risk control of HMs for different land uses. However, the health risks of HMs in the study area cannot be ignored. If timely measures are not applied, it will threaten human health in the region for a long time.

### Conclusion and environmental impact

This study analyzed the pollution characteristics, sources, and health risks of HMs in soils with different land uses in a typical industrial and mining city in the Hexi Corridor of China. The main conclusions are as follows:

Due to long-term industrial activities such as mining and smelting, Cu, Zn, Ni, Pb, and Cd accumulated in the soil, among which Cu and Ni were the most polluted.

The PMF model divided the sources of HMs in the study area into three pollution sources: Pb—traffic emissions (32.58%), Cu and Ni—industrial activities (55.79%), and Zn and Cd—agricultural activities (11.63%).

The combined characterization techniques of XRD, STEM-EDS, and XPS proved that the HMs from smelter waste were transferred to soil.

Monte Carlo simulation of health risk assessment results showed that HMs in all land-use soils held non-carcinogenic and carcinogenic risks for children and adults, and measures were needed to control HM health risk pollution. Of concern is that Ni in the soils of farmland, woodland, grassland, and green belt contributes more than 90% of the cancer risk to children and adults.

Finally, the PMF and HAR models were combined to explore the contribution of pollution sources to the health risk posed by HMs in the soils with different land uses. It was found that industrial activities mainly controlled the non-carcinogenic and carcinogenic risks to children and adults.

With the rapid development of urbanization, the results of this study have guiding significance for risk control of HMs in soils with different land uses from the source and can better prevent and reduce the risk of HMs to human health. In addition, at the level of urban soil HM prevention and control, parks, primitive forests, and other areas can be considered HM background points.

**Author Contributions** JX helped in conceptualization, methodology, data collection and analysis, writing the original draft. YW was involved in performing the experiment, investigation, revision of the original draft. SW contributed to review, conceptualization, resources, supervision. YW and SD helped in performing the experiment and treatment of samples. ZC performed soil sampling and treatment of samples. LH investigated and visualized the study.

**Funding** This work was supported by the National Key Research and Development Program of China (2018YFC1802905).

**Data Availability** The datasets used or analyzed during the current study are available from the corresponding author on reasonable request.

### Declarations

**Competing interests** The authors declare they have no conflict of interests.

### References

- Adamo, P., Iavazzo, P., Albanese, S., Agrelli, D., De Vivo, B., & Lima, A. (2014). Bioavailability and soil-to-plant transfer factors as indicators of potentially toxic element contamination in agricultural soils. *Science of the Total Environment*, 500–501, 11–22. <https://doi.org/10.1016/j.scitotenv.2014.08.085>
- Ağca, N., & Özdel, E. (2014). Assessment of spatial distribution and possible sources of heavy metals in the soils of Sariseki-Dörtyol District in Hatay Province (Turkey). *Environmental Earth Sciences*, 71, 1033–1047. <https://doi.org/10.1007/s12665-013-2507-8>
- Almeida-Silva, M., Almeida, S. M., Freitas, M. C., Pio, C. A., Nunes, T., & Cardoso, J. (2013). Impact of Sahara Dust Transport on Cape Verde Atmospheric Element Particles. *Journal of Toxicology and Environmental Health Part A*, 76, 240–251. <https://doi.org/10.1080/15287394.2013.757200>
- Anaman, R., Peng, C., Jiang, Z., Liu, X., Zhou, Z., Guo, Z., & Xiao, X. (2022). Identifying sources and transport routes of heavy metals in soil with different land uses around a smelting site by GIS based PCA and PMF. *Science of the Total Environment*, 823, 153759. <https://doi.org/10.1016/j.scitotenv.2022.153759>



- Başaran, B. (2022). Comparison of heavy metal levels and health risk assessment of different bread types marketed in Turkey. *Journal of Food Composition and Analysis*, 108, 104443. <https://doi.org/10.1016/j.jfca.2022.104443>
- Bisht, L., Gupta, V., Singh, A., Gautam, A. S., & Gautam, S. (2022). Heavy metal concentration and its distribution analysis in urban road dust: A case study from most populated city of Indian state of Uttarakhand. *Spatial and Spatio-Temporal Epidemiology*, 40, 100470. <https://doi.org/10.1016/j.sste.2021.100470>
- Cai, J., Wang, J., Zhang, Y., Tian, H., Zhu, C., Gross, D. S., Hu, M., Hao, J., He, K., Wang, S., & Zheng, M. (2017). Source apportionment of Pb-containing particles in Beijing during January 2013. *Environmental Pollution*, 226, 30–40. <https://doi.org/10.1016/j.envpol.2017.04.004>
- Cai, L.-M., Wang, Q.-S., Luo, J., Chen, L.-G., Zhu, R.-L., Wang, S., & Tang, C.-H. (2019). Heavy metal contamination and health risk assessment for children near a large Cu-smelter in central China. *Science of the Total Environment*, 650, 725–733. <https://doi.org/10.1016/j.scitotenv.2018.09.081>
- Chen, H., Teng, Y., Chen, R., Li, J., & Wang, J. (2016). Contamination characteristics and source apportionment of trace metals in soils around Miyun Reservoir. *Environmental Science and Pollution Research*, 23, 15331–15342. <https://doi.org/10.1007/s11356-016-6694-1>
- Chen, H., Wang, L., Hu, B., Xu, J., & Liu, X. (2022). Potential driving forces and probabilistic health risks of heavy metal accumulation in the soils from an e-waste area, southeast China. *Chemosphere*, 289, 133182. <https://doi.org/10.1016/j.chemosphere.2021.133182>
- Christophoridis, C., Dedepsidis, D., & Fytianos, K. (2009). Occurrence and distribution of selected heavy metals in the surface sediments of Thermaikos Gulf, N. Greece. Assessment using pollution indicators. *Journal of Hazardous Materials*, 168, 1082–1091. <https://doi.org/10.1016/j.jhazmat.2009.02.154>
- CNEMC (China National Environmental Monitoring Center). (1995). *The Background Value of Soil Elements of China*. China Environmental Science Press.
- Crundwell, F. K., Moats, M. S., Ramachandran, V., Robinson, T. G., & Davenport, W. G. (2011). Chapter 17 - Smelting of Nickel Sulfide Concentrates by Roasting and Electric Furnace Smelting. In F. K. Crundwell, M. S. Moats, V. Ramachandran, T. G. Robinson, & W. G. Davenport (Eds.), *Extractive Metallurgy of Nickel Cobalt and Platinum Group Metals* (pp. 199–214). Elsevier.
- Ding, H., Nan, Z., Liu, X., Li, Y., Wang, S., Qin, S., & Zhao, Z. (2008). Contamination characteristics of heavy metals in agricultural soils on the outskirts of Jinchang city. *Journal of Agro-Environmental Scienc*, 27, 2183–2188. <https://doi.org/10.3321/j.issn:1672-2043.2008.06.010>
- Dutta, D., Goel, S., & Kumar, S. (2022). Health risk assessment for exposure to heavy metals in soils in and around E-waste dumping site. *Journal of Environmental Chemical Engineering*, 10, 107269. <https://doi.org/10.1016/j.jece.2022.107269>
- EPA, U. 1996. Soil screening guidance: Technical background document. Superfund | US EPA.
- Fan, X., Lu, X., Yu, B., Zuo, L., Fan, P., Yang, Y., Zhuang, S., Liu, H., & Qin, Q. (2021). Risk and sources of heavy metals and metalloids in dust from university campuses: A case study of Xi'an. *China. Environmental Research*, 202, 111703. <https://doi.org/10.1016/j.envres.2021.111703>
- Fei, X., Lou, Z., Xiao, R., Ren, Z., & Lv, X. (2020). Contamination assessment and source apportionment of heavy metals in agricultural soil through the synthesis of PMF and GeogDetector models. *Science of the Total Environment*, 747, 141293. <https://doi.org/10.1016/j.scitotenv.2020.141293>
- Fei, X., Lou, Z., Xiao, R., Ren, Z., & Lv, X. (2022). Source analysis and source-oriented risk assessment of heavy metal pollution in agricultural soils of different cultivated land qualities. *Journal of Cleaner Production*, 341, 130942. <https://doi.org/10.1016/j.jclepro.2022.130942>
- Gautam, A., Sharma, P. K., Baredar, P., Warudkar, V., Bhagoria, J. L., & Ahmed, S. (2021). Modeling of atmospheric boundary flows using experimental investigation over complex terrain in a non-neutral condition. *Materials Today: Proceedings*, 46, 5681–5686. <https://doi.org/10.1016/j.matpr.2020.09.735>
- Gautam, A., Warudkar, V., & Bhagoria, J. L. (2022). A comparative analysis of wind characteristics for distinct terrains of India. *Sustainable Energy Technologies and Assessments*, 52, 102089. <https://doi.org/10.1016/j.seta.2022.102089>
- Gautam, S. B. J. (2020). Spatio-temporal variation in the concentration of atmospheric particulate matter: A study in fourth largest urban agglomeration in India. *Environmental Technology & Innovation*, 17, 100546. <https://doi.org/10.1016/j.eti.2019.100546>
- Gopinathan, P., Jha, M., Singh, A. K., Mahato, A., Subramani, T., Singh, P. K., & Singh, V. (2022a). Geochemical characteristics, origin and forms of sulphur distribution in the Talcher coalfield. *India. Fuel*, 316, 123376. <https://doi.org/10.1016/j.fuel.2022.123376>
- Gopinathan, P., Santosh, M. S., Dileepkumar, V. G., Subramani, T., Reddy, R., Masto, R. E., & Maity, S. (2022b). Geochemical, mineralogical and toxicological characteristics of coal fly ash and its environmental impacts. *Chemosphere*, 307, 135710. <https://doi.org/10.1016/j.chemosphere.2022.135710>
- Gopinathan, P., Singh, A. K., Singh, P. K., & Jha, M. (2022c). Sulphur in Jharia and Raniganj coalfields: Chemical fractionation and its environmental implications. *Environmental Research*, 204, 112382. <https://doi.org/10.1016/j.envres.2021.112382>
- Gu, X., Wang, Z., Wang, J., Ouyang, W., Wang, B., Xin, M., Lian, M., Lu, S., Lin, C., He, M., & Liu, X. (2022). Sources, trophodynamics, contamination and risk assessment of toxic metals in a coastal ecosystem by using a receptor model and Monte Carlo simulation. *Journal of Hazardous Materials*, 424, 127482. <https://doi.org/10.1016/j.jhazmat.2021.127482>
- Guan, Q., Cai, A., Wang, F., Yang, L., Xu, C., & Liu, Z. (2017). Spatio-temporal variability of particulate matter in the key part of Gansu Province, Western China. *Environmental Pollution*, 230, 189–198. <https://doi.org/10.1016/j.envpol.2017.06.045>
- Guan, Q., Wang, F., Xu, C., Pan, N., Lin, J., Zhao, R., Yang, Y., & Luo, H. (2018). Source apportionment of heavy metals in agricultural soil based on PMF: A case study in Hexi

- Corridor, northwest China. *Chemosphere*, 193, 189–197. <https://doi.org/10.1016/j.chemosphere.2017.10.151>
- Guan, Q., Zhao, R., Pan, N., Wang, F., Yang, Y., & Luo, H. (2019). Source apportionment of heavy metals in farmland soil of Wuwei, China: Comparison of three receptor models. *Journal of Cleaner Production*, 237, 117792. <https://doi.org/10.1016/j.jclepro.2019.117792>
- Guppy, C. N., Menzies, N. W., Moody, P. W., & Blamey, F. (2005). Competitive sorption reactions between phosphorus and organic matter in soil: A review. *Soil Research*, 43, 189–202. <https://doi.org/10.1071/SR04049>
- Gupta, D. K., Chatterjee, S., Datta, S., Veer, V., & Walther, C. (2014). Role of phosphate fertilizers in heavy metal uptake and detoxification of toxic metals. *Chemosphere*, 108, 134–144. <https://doi.org/10.1016/j.chemosphere.2014.01.030>
- Haghnazar, H., Johannesson, K. H., González-Pinzón, R., Pourakbar, M., Aghayani, E., Rajabi, A., & Hashemi, A. A. (2022). Groundwater geochemistry, quality, and pollution of the largest lake basin in the Middle East: Comparison of PMF and PCA-MLR receptor models and application of the source-oriented HHRA approach. *Chemosphere*, 288, 132489. <https://doi.org/10.1016/j.chemosphere.2021.132489>
- Hu, B., Jia, X., Hu, J., Xu, D., & Xia, F. (2017). Assessment of heavy metal pollution and health risks in the soil-plant-human system in the Yangtze River Delta, China. *International Journal of Environmental Research & Public Health*, 14, 1–18. <https://doi.org/10.3390/ijerph14091042>
- Hu, X., Nan, Z., Liu, X., Li, Y., & Ding, H. (2011). Study on the distribution characteristics of soil heavy metals in urban residential areas of Jinchang. *Journal of Arid Land Resources and Environment*, 25, 180–184.
- Huang, J., Guo, S., Zeng, G.-M., Li, F., Gu, Y., Shi, Y., Shi, L., Liu, W., & Peng, S. (2018). A new exploration of health risk assessment quantification from sources of soil heavy metals under different land use. *Environmental Pollution*, 243, 49–58. <https://doi.org/10.1016/j.envpol.2018.08.038>
- Huang, J., Nan, Z., Liu, X., Li, Y., & Ding, H. (2010). Characteristics of heavy metal content and pollution evaluation of urban green belt soil in Jinchang City. *Journal of Arid Land Resources and Environment*, 24, 187–191.
- Huang, J., Wu, Y., Sun, J., Li, X., Geng, X., Zhao, M., Sun, T., & Fan, Z. (2021). Health risk assessment of heavy metal(loid)s in park soils of the largest megacity in China by using Monte Carlo simulation coupled with Positive matrix factorization model. *Journal of Hazardous Materials*, 415, 125629. <https://doi.org/10.1016/j.jhazmat.2021.125629>
- Jiang, Y., Wei, X., He, H., She, J., Liu, J., Fang, F., Zhang, W., Liu, Y., Wang, J., Xiao, T., & Tsang, D. C. W. (2022). Transformation and fate of thallium and accompanying metal(loid)s in paddy soils and rice: A case study from a large-scale industrial area in China. *Journal of Hazardous Materials*, 423, 126997. <https://doi.org/10.1016/j.jhazmat.2021.126997>
- Jing, L., Yong, J., Zhe, N. A., & Zhang. (2018). Quantitative contributions of the major sources of heavy metals in soils to ecosystem and human health risks: A case study of Yulin, China. *Ecotoxicology and Environmental Safety*, 164, 261–269. <https://doi.org/10.1016/j.ecoenv.2018.08.030>
- Kavdir, Y., & Killi, D. (2008). Influence of olive oil solid waste applications on soil pH, electrical conductivity, soil nitrogen transformations, carbon content and aggregate stability. *Bioresource Technology*, 99, 2326–2332. <https://doi.org/10.1016/j.biortech.2007.05.034>
- Kennedy, C., Pincetl, S., & Bunje, P. (2011). The study of urban metabolism and its applications to urban planning and design. *Environmental Pollution*, 159, 1965–1973. <https://doi.org/10.1016/j.envpol.2010.10.022>
- Khuzestani, R. B., & Souri, B. (2013). Evaluation of heavy metal contamination hazards in nuisance dust particles, in Kurdistan Province, western Iran. *Journal of Environmental Sciences*, 25, 1346–1354. [https://doi.org/10.1016/S1001-0742\(12\)60147-8](https://doi.org/10.1016/S1001-0742(12)60147-8)
- Kratz, S., Schick, J., & Schnug, E. (2016). Trace elements in rock phosphates and P containing mineral and organo-mineral fertilizers sold in Germany. *Science of the Total Environment*, 542, 1013–1019. <https://doi.org/10.1016/j.scitotenv.2015.08.046>
- Kulikowska, D., Gusiati, Z. M., Bułkowska, K., & Klik, B. (2015). Feasibility of using humic substances from compost to remove heavy metals (Cd, Cu, Ni, Pb, Zn) from contaminated soil aged for different periods of time. *Journal of Hazardous Materials*, 300, 882–891. <https://doi.org/10.1016/j.jhazmat.2015.08.022>
- Lee, C.S.-L., Li, X., Shi, W., Cheung, S.C.-N., & Thornton, I. (2006). Metal contamination in urban, suburban, and country park soils of Hong Kong: A study based on GIS and multivariate statistics. *Science of the Total Environment*, 356, 45–61. <https://doi.org/10.1016/j.scitotenv.2005.03.024>
- Lefticariu, L., Sutton, S. R., Bender, K. S., Lefticariu, M., Pentrak, M., & Stucki, J. W. (2017). Impacts of detrital nano- and micro-scale particles (dNP) on contaminant dynamics in a coal mine AMD treatment system. *Science of the Total Environment*, 575, 941–955. <https://doi.org/10.1016/j.scitotenv.2016.09.154>
- Li, R., Zhang, H., Wang, F., Ren, Y., Jia, S., Jiang, B., Jia, X., Tang, Y., & Tang, M. (2022a). Abundance and fractional solubility of phosphorus and trace metals in combustion ash and desert dust: Implications for bioavailability and reactivity. *Science of the Total Environment*, 816, 151495. <https://doi.org/10.1016/j.scitotenv.2021.151495>
- Li, X., Liu, H., Meng, W., Liu, N., & Wu, P. (2022b). Accumulation and source apportionment of heavy metal(loid)s in agricultural soils based on GIS, SOM and PMF: A case study in superposition areas of geochemical anomalies and zinc smelting, Southwest China. *Process Safety and Environmental Protection*, 159, 964–977. <https://doi.org/10.1016/j.psep.2022.01.072>
- Li, Y., Beeton, R. J. S., Halog, A., & Sigler, T. (2016). Evaluating urban sustainability potential based on material flow analysis of inputs and outputs: A case study in Jinchang City, China. *Resources, Conservation and Recycling*, 110, 87–98. <https://doi.org/10.1016/j.resconrec.2016.03.023>
- Lian, Z., Zhao, X., Gu, X., Li, X., Luan, M., & Yu, M. (2022). Presence, sources, and risk assessment of heavy metals in the upland soils of northern China using Monte Carlo

- simulation. *Ecotoxicology and Environmental Safety*, 230, 113154. <https://doi.org/10.1016/j.ecoenv.2021.113154>
- Liu, E., Yan, T., Birch, G., & Zhu, Y. (2014). Pollution and health risk of potentially toxic metals in urban road dust in Nanjing, a mega-city of China. *Science of the Total Environment*, 476–477, 522–531. <https://doi.org/10.1016/j.scitotenv.2014.01.055>
- Liu, J., Li, N., Zhang, W., Wei, X., Tsang, D. C. W., Sun, Y., Luo, X., a Bao, Z., Zheng, W., Wang, J., Xu, G., Hou, L., Chen, Y., & Feng, Y. (2019). Thallium contamination in farmlands and common vegetables in a pyrite mining city and potential health risks. *Environmental Pollution*, 248, 906–915. <https://doi.org/10.1016/j.envpol.2019.02.092>
- Liu, P., Wu, Q., Wang, X., Hu, W., Liu, X., Tian, K., n fan, Y., Xie, E., Zhao, Y., Huang, B., Yoon, S. J., Kwon, B.-O., & Khim, J. S. (2022). Spatiotemporal variation and sources of soil heavy metals along the lower reaches of Yangtze River. *China. Chemosphere*, 291, 132768. <https://doi.org/10.1016/j.chemosphere.2021.132768>
- Lu, X., Wang, L., Lei, K., Huang, J., & Zhai, Y. (2009). Contamination assessment of copper, lead, zinc, manganese and nickel in street dust of Baoji, NW China. *Journal of Hazardous Materials*, 161, 1058–1062. <https://doi.org/10.1016/j.jhazmat.2008.04.052>
- Luo, H., Wang, Q., Guan, Q., Ma, Y., Ni, F., Yang, E., & Zhang, J. (2022). Heavy metal pollution levels, source apportionment and risk assessment in dust storms in key cities in Northwest China. *Journal of Hazardous Materials*, 422, 126878. <https://doi.org/10.1016/j.jhazmat.2021.126878>
- Ma, W., Tai, L., Qiao, Z., Zhong, L., Wang, Z., Fu, K., & Chen, G. (2018). Contamination source apportionment and health risk assessment of heavy metals in soil around municipal solid waste incinerator: A case study in North China. *Science of the Total Environment*, 631–632, 348–357. <https://doi.org/10.1016/j.scitotenv.2018.03.011>
- Paatero, P., & Tapper, U. (1993). Analysis of different modes of factor analysis as least squares fit problems. *Chemometrics and Intelligent Laboratory Systems*, 18, 183–194. [https://doi.org/10.1016/0169-7439\(93\)80055-M](https://doi.org/10.1016/0169-7439(93)80055-M)
- Pirsaheb, M., Hadei, M., & Sharafi, K. (2021). Human health risk assessment by Monte Carlo simulation method for heavy metals of commonly consumed cereals in Iran-Uncertainty and sensitivity analysis. *Journal of Food Composition and Analysis*, 96, 103697. <https://doi.org/10.1016/j.jfca.2020.103697>
- Qu, M.-K., Li, W.-D., Zhang, C.-R., Wang, S.-Q., Yang, Y., & He, L.-Y. (2013). Source Apportionment of Heavy Metals in Soils Using Multivariate Statistics and Geostatistics. *Pedosphere*, 23, 437–444. [https://doi.org/10.1016/S1002-0160\(13\)60036-3](https://doi.org/10.1016/S1002-0160(13)60036-3)
- Ren, Y., Luo, Q., Zhuo, S., Hu, Y., Shen, G., Cheng, H., & Tao, S. (2021). Bioaccessibility and public health risk of heavy Metal(loid)s in the airborne particulate matter of four cities in northern China. *Chemosphere*, 277, 130312. <https://doi.org/10.1016/j.chemosphere.2021.130312>
- Shao, D., Zhan, Y., Zhou, W., & Zhu, L. (2016). Current status and temporal trend of heavy metals in farmland soil of the Yangtze River Delta Region: Field survey and meta-analysis. *Environmental Pollution*, 219, 329–336. <https://doi.org/10.1016/j.envpol.2016.10.023>
- Sharma, P. K., Gautam, A., Warudkar, V., Ahmed, S., & Bhagoria, J. L. (2021). Analysis of wind characteristics parameters with the application of lidar and mast. *Wind Energy*, 24, 413–427. <https://doi.org/10.1002/we.2580>
- Shen, D., Huang, S., Zhang, Y., & Zhou, Y. (2021). The source apportionment of N and P pollution in the surface waters of lowland urban area based on EEM-PAR-AFAC and PCA-APCS-MLR. *Environmental Research*, 197, 111022. <https://doi.org/10.1016/j.envres.2021.111022>
- Shentu, J., Li, X., Han, R., Chen, Q., Shen, D., & Qi, S. (2022). Effect of site hydrological conditions and soil aggregate sizes on the stabilization of heavy metals (Cu, Ni, Pb, Zn) by biochar. *Science of the Total Environment*, 802, 149949. <https://doi.org/10.1016/j.scitotenv.2021.149949>
- Shi, W., Li, T., Feng, Y., Su, H., & Yang, Q. (2022). Source apportionment and risk assessment for available occurrence forms of heavy metals in Dongdahe Wetland sediments, southwest of China. *Science of the Total Environment*, 815, 152837. <https://doi.org/10.1016/j.scitotenv.2021.152837>
- Smichowski, P., Gómez, D., Frazzoli, C., & Caroli, S. (2007). Traffic-related elements in airborne particulate matter. *Applied Spectroscopy Reviews*, 43, 23–49. <https://doi.org/10.1080/05704920701645886>
- Sobanska, S., Deneele, D., Barbillat, J., & Ledésert, B. (2016). Natural weathering of slags from primary Pb–Zn smelting as evidenced by Raman microspectroscopy. *Applied Geochemistry*, 64, 107–117. <https://doi.org/10.1016/j.apgeochem.2015.09.011>
- Sohn, H. Y., Kang, S., & Chang, J. (2005). Sulfide smelting fundamentals, technologies and innovations. *Mining, Metallurgy & Exploration*, 22, 65–76. <https://doi.org/10.1007/BF03403117>
- Sutherland, R. A. (2000). Bed sediment-associated trace metals in an urban stream, Oahu. *Hawaii. Environmental Geology*, 39, 611–627. <https://doi.org/10.1007/s002540050473>
- Tao, Y., An, X., Sun, Z., Hou, Q., & Wang, Y. (2012). Association between dust weather and number of admissions for patients with respiratory diseases in spring in Lanzhou. *Science of the Total Environment*, 423, 8–11. <https://doi.org/10.1016/j.scitotenv.2012.01.064>
- Tian, K., Li, M., Hu, W., & Y. n. Fan, B. Huang, Y. Zhao. (2022). Environmental capacity of heavy metals in intensive agricultural soils: Insights from geochemical base-lines and source apportionment. *Science of the Total Environment*, 819, 153078. <https://doi.org/10.1016/j.scitotenv.2022.153078>
- Tong, Z. (2012). Study on the Characteristics of Heavy Metal Pollution in Particulate Matter in Jinchang City. *Gansu Science and Technology*, 28, 34–36.
- USEPA. 2014. EPA Positive Matrix Factorization (PMF) 5.0 Fundamentals and User Guide [WWW Document].
- Vodyanitskii, Y. N., & Shoba, S. A. (2015). Magnetic susceptibility as an indicator of heavy metal contamination of urban soils (Review). *Moscow University Soil Science Bulletin*, 70, 10–16. <https://doi.org/10.3103/S014768741501007X>
- Wang, F., Guan, Q., Tian, J., Lin, J., Yang, Y., Yang, L., & Pan, N. (2020). Contamination characteristics, source apportionment, and health risk assessment of heavy metals

- in agricultural soil in the Hexi Corridor. *CATENA*, 191, 104573. <https://doi.org/10.1016/j.catena.2020.104573>
- Wang, J., Su, J., Li, Z., Liu, B., Cheng, G., Jiang, Y., Li, Y., Zhou, S., & Yuan, W. (2019). Source apportionment of heavy metal and their health risks in soil-dustfall-plant system nearby a typical non-ferrous metal mining area of Tongling, Eastern China. *Environ Pollut*, 254, 113089. <https://doi.org/10.1016/j.envpol.2019.113089>
- Wang, Y., Guo, G., Zhang, D., & Lei, M. (2021). An integrated method for source apportionment of heavy metal(oid)s in agricultural soils and model uncertainty analysis. *Environmental Pollution*, 276, 116666. <https://doi.org/10.1016/j.envpol.2021.116666>
- Wu, Y., Li, X., Yu, L., Wang, T., Wang, J., & Liu, T. (2022). Review of soil heavy metal pollution in China: Spatial distribution, primary sources, and remediation alternatives. *Resources, Conservation and Recycling*, 181, 106261. <https://doi.org/10.1016/j.resconrec.2022.106261>
- Xiaohu, L., Neutral, T., & Fengyou, C. (2009). Transport characteristics of heavy metals in soils around copper-nickel mining areas in Jinchang. *Journal of Jilin University: Earth Science Edition*, 39, 131–136. <https://doi.org/10.3969/j.issn.1671-5888.2009.01.020>
- Xiaona, H., Zhongren, N., Xiaowen, L., Yuan, L., & Haixia, D. (2011). Study on the distribution characteristics of heavy metals in urban residential areas of Jinchang. *Arid Zone Resources and Environment*, 25, 180–184.
- Xing, W., & Ma, D. (2021). Study on the path of promoting high-quality development of modern special agricultural industry of vegetables, grasses and livestock: the case of Jinchang City, Gansu Province. *Village Technology*, 12, 40–42.
- Xu, D.-M., & Fu, R.-B. (2022). A typical case study from smelter-contaminated soil: New insights into the environmental availability of heavy metals using an integrated mineralogy characterization. *Environmental Science and Pollution Research*. <https://doi.org/10.1007/s11356-022-19823-6>
- Xu, D.-M., Fu, R.-B., Wang, J.-X., & An, B.-H. (2022). The geochemical behaviors of potentially toxic elements in a typical lead/zinc (Pb/Zn) smelter contaminated soil with quantitative mineralogical assessments. *Journal of Hazardous Materials*, 424, 127127. <https://doi.org/10.1016/j.jhazmat.2021.127127>
- Xu, D.-M., Yan, B., Chen, T., Lei, C., Lin, H.-Z., & Xiao, X.-M. (2017). Contaminant characteristics and environmental risk assessment of heavy metals in the paddy soils from lead (Pb)-zinc (Zn) mining areas in Guangdong Province, South China. *Environmental Science and Pollution Research*, 24, 24387–24399. <https://doi.org/10.1007/s11356-017-0052-9>
- Xu, J., Li, Y., Wang, S., Long, S., Wu, Y., & Chen, Z. (2023). Sources, transfers and the fate of heavy metals in soil-wheat systems: The case of lead (Pb)/zinc (Zn) smelting region. *Journal of Hazardous Materials*, 441, 129863. <https://doi.org/10.1016/j.jhazmat.2022.129863>
- Yongsohn, H. (2014). Chapter 2.1 - Copper Production. In S. Seetharaman (Ed.), *Treatise on Process Metallurgy* (pp. 534–624). Elsevier.
- Yuan, L., Zhongren, N., Xiaowen, L., Shengli, W., & Haixia, D. (2009). Distribution patterns of heavy metals Cu, Zn and Ni in suburban cultivated soils of Jinchang. *Arid Zone Resources and Environment*, 23, 164–170.
- Zang, F., Wang, S., Nan, Z., Ma, J., Li, Y., Zhang, Q., & Chen, Y. (2017a). Immobilization of Cu, Zn, Cd and Pb in mine drainage stream sediment using Chinese loess. *Chemosphere*, 181, 83–91. <https://doi.org/10.1016/j.chemosphere.2017.04.070>
- Zang, F., Wang, S., Nan, Z., Ma, J., Zhang, Q., Chen, Y., & Li, Y. (2017b). Accumulation, spatio-temporal distribution, and risk assessment of heavy metals in the soil-corn system around a polymetallic mining area from the Loess Plateau, northwest China. *Geoderma*, 305, 188–196. <https://doi.org/10.1016/j.geoderma.2017.06.008>
- Zhang, J., Li, H., Zhou, Y., Dou, L., Cai, L., Mo, L., & You, J. (2018). Bioavailability and soil-to-crop transfer of heavy metals in farmland soils: A case study in the Pearl River Delta, South China. *Environmental Pollution*, 235, 710–719. <https://doi.org/10.1016/j.envpol.2017.12.106>
- Zhang, Y., Guo, Z., Peng, C., Deng, H., & Xiao, X. (2021a). A questionnaire based probabilistic risk assessment (PRA) of heavy metals in urban and suburban soils under different land uses and receptor populations. *Science of the Total Environment*, 793, 148525. <https://doi.org/10.1016/j.scitotenv.2021.148525>
- Zhang, Y., Wang, S., Gao, Z., Zhang, H., Zhu, Z., Jiang, B., Liu, J., & Dong, H. (2021b). Contamination characteristics, source analysis and health risk assessment of heavy metals in the soil in Shi River Basin in China based on high density sampling. *Ecotoxicology and Environmental Safety*, 227, 112926. <https://doi.org/10.1016/j.ecoenv.2021.112926>
- Zhao, T. (2012). Study on the characteristics of heavy metal pollution in particulate matter in Jinchang City. *Gansu Science and Technology*, 28, 34–36. <https://doi.org/10.3969/j.issn.1000-0952.2012.06.013>
- Zhou, Y., Wang, L., Xiao, T., Chen, Y., Beiyuan, J., She, J., Zhou, Y., Yin, M., Liu, J., Liu, Y., Wang, Y., & Wang, J. (2020). Legacy of multiple heavy metal(oid)s contamination and ecological risks in farmland soils from a historical artisanal zinc smelting area. *Science of the Total Environment*, 720, 137541. <https://doi.org/10.1016/j.scitotenv.2020.137541>
- Zhuang, P., Li, Z. A., Zou, B., Xia, H.-P., & Wang, G. (2013). Heavy metal contamination in soil and Soybean near the Dabaoshan Mine, South China. *Pedosphere*, 23, 298–304. [https://doi.org/10.1016/S1002-0160\(13\)60019-3](https://doi.org/10.1016/S1002-0160(13)60019-3)

**Publisher's Note** Springer Nature remains neutral with regard to jurisdictional claims in published maps and institutional affiliations.

Springer Nature or its licensor (e.g. a society or other partner) holds exclusive rights to this article under a publishing agreement with the author(s) or other rightsholder(s); author self-archiving of the accepted manuscript version of this article is solely governed by the terms of such publishing agreement and applicable law.